Comprehensive Experimental and Theoretical Study into the Complete Valence Electronic Structure of Norbornadiene

H. Mackenzie-Ross,[†] M. J. Brunger,*[,†] F. Wang,[‡] W. Adcock,[†] T. Maddern,[†] L. Campbell,[†] W. R. Newell,[†,§] I. E. McCarthy,[†] E. Weigold,[||] B. Appelbe,[‡] and D. A. Winkler[⊥]

School of Chemistry, Physics and Earth Sciences, The Flinders University of South Australia, GPO Box 2100, Adelaide, SA 5001, Australia, VPAC, 110 Victoria Street, PO Box 201, Carlton South, Victoria 3053, Australia, Department of Physics and Astronomy, University College London, Gower Street, London, United Kingdom WC1E 6BT, Research School of Physical Science and Engineering, Australian National University, Canberra, ACT 0200, Australia, and CSIRO Division of Molecular Sciences, Private Bag 10, Clayton South MDC, Victoria 3169, Australia

Received: June 5, 2002; In Final Form: August 12, 2002

Momentum Distributions (MDs), obtained using high-resolution electron momentum spectroscopy (HREMS), are reported for norbornadiene's 18 valence orbitals. Corresponding theoretical results, using generalized gradient approximation density functional theory (DFT) together with TZVP, DZVP, and DZVP2 basis functions and a plane wave impulse approximation to describe the ionization process, are also detailed. This work represents the first comprehensive HREMS/DFT investigation into the complete valence electronic structure of norbornadiene (NBD), with significant results being obtained. In particular, an exacting comparison between our experimental and theoretical MDs enables us to define the "optimum" basis for NBD, from those we studied. This "optimum" basis is then used to extract a wide range of NBD's important molecular property information, which are subsequently compared with the results of independent measurements and calculations. Agreement between our results and those from independent measurements was generally very good, highlighting the utility of HREMS in a priori basis set evaluation.

1. Introduction

High-resolution electron momentum spectroscopy (HREMS), or (e,2e) coincidence spectroscopy, is now a well-developed tool for the investigation of the valence electronic structure of molecules due to its unique ability to measure the orbital momentum distribution (MD) for binding-energy-selected electrons.[1] Furthermore, within the plane wave impulse approximation (PWIA) and, in many cases, the target Hartree−Fock (THFA) or target Kohn−Sham (TKSA) approximations,[2] this measured MD may be directly compared with the calculated spherically averaged MD of a specific molecular orbital (MO), once the appropriate angular resolution has been folded in.[3] Hence, HREMS is also a powerful technique for evaluating the quality of theoretical wave functions in quantum chemistry,[4] and in this paper we report its application to norbornadiene (NBD).

Our original interest in the electronic structure of NBD (bicyclo[2.2.1]-heptadiene; C_7H_8) was due to it being the prototypical molecule for the study of through-space and through-bond interaction, concepts originally introduced by Hoffmann and colleagues[5−7] and incorporated into an SCF scheme by Heilbronner and Schmelzer.[8] The ability of HREMS to unambiguously identify the symmetry of an orbital from its measured MD, thus made it the ideal technique to definitively determine the dominant interaction between NBD's outermost π orbitals. The results from that study are reported elsewhere,[9] although we note here that the through-space interaction was found to dominate.

While conducting the above study,[9] it became quite clear that existing investigations into the complete valence electronic structure of NBD (and not just the highest-occupied-molecular-orbital [HOMO] and next-highest-occupied-molecular-orbital [NHOMO]) are rather restricted. Previous photoelectron spectroscopy (PES) studies include the He (I) measurement from Bischof et al.[10] and the He (II) measurement from Bieri et al.[11] Their observed spectra were interpreted by von Niessen and Diercksen,[12] using an ab initio many-body Green's function method. The results they found were consistent with those put forward earlier by Heilbronner and Martin[13] although, as noted by both von Niessen and Diercksen[12] and Galasso,[14] the ordering of the orbital energies was not uniformly reproduced by all of the calculations.[6,12,15−17] The original EMS study[18] on NBD reported MDs for only its HOMO and NHOMO. That work was conducted at a total energy of 1200 eV and with a modest energy resolution (ΔE_{coin}) of 1.5 eV (fwhm). Unfortunately, the HOMO and NHOMO in NBD are only separated by 0.85 eV,[10,11] so that Takahashi et al.[18] could not resolve them in their binding-energy spectra. In addition, with this broad energy resolution, contributions from the adjacent $2a_2$ orbital to the NHOMO and even HOMO flux could also not be ruled out. To try and circumvent these difficulties, Takahashi et al.[18] used a spectral deconvolution procedure, but the uniqueness of this procedure is debateable in this case as is reflected by the scatter in their MD data.[9] Consequently, we have made new HREMS measurements ($\Delta E_{coin} \approx 0.55$ eV, fwhm) to improve the quality

[†] School of Chemistry, Physics and Earth Sciences, The Flinders University of South Australia.
[‡] VPAC.
[§] Department of Physics and Astronomy, University College London.
[||] Research School of Physical Science and Engineering, Australian National University.
[⊥] CSIRO Division of Molecular Sciences.

10.1021/jp021338d CCC: $22.00
Published on Web 09/17/2002

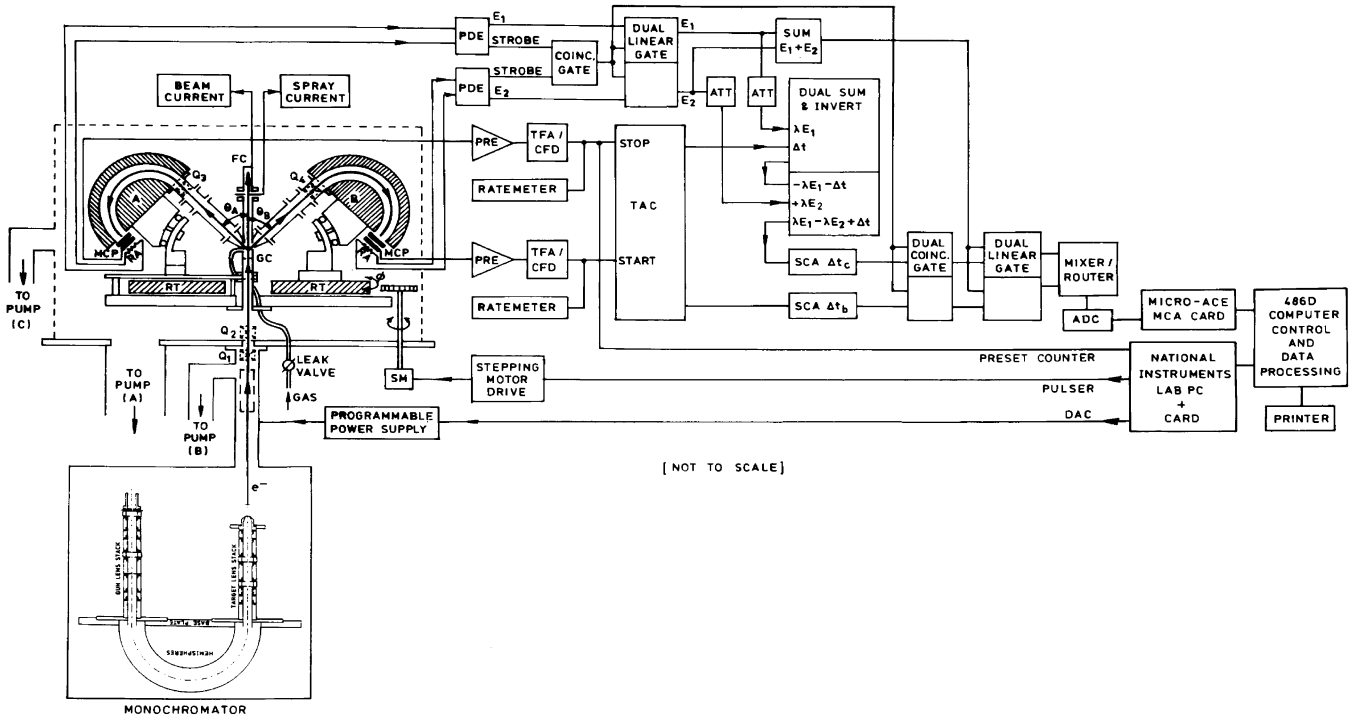

Figure 1. Schematic diagram of the Flinders symmetric noncoplanar HREMS spectrometer.

of the available HOMO and NHOMO MD data, as well as significantly extend the scope of the original investigation to report MDs for norbornadiene's 16 other valence orbitals. When coupled with our PWIA and density functional theory (DFT) calculations, our present study quite possibly represents the most comprehensive investigation into NBD's electronic structure that has yet been performed.

Contrary to the situation described immediately above for the electronic structure of NBD, experimental and theoretical studies into its physicochemical properties have been more prevalent. They include molecular geometry experiments[19,20] and calculations,[21−23] infrared and Raman spectroscopy results[24] and NMR results.[25] More recently, Penning ionization electron spectroscopy (PIES) data[26] has also become available.

In section 2, we briefly discuss some of the experimental aspects of the HREMS technique, whereas in section 3, details of our structure calculations are provided. The results of the experimental and theoretical MDs are presented and discussed in detail in section 4. The significance of the present application of HREMS to NBD is that by comparing the experimental and theoretical MDs, for the relevant valence orbitals, we can independently determine which of the DFT basis sets we have studied provides the most physically reasonable representation of the NBD molecule. Standard UniChem[27,28] features then allow us to utilize this "optimum" wave function to extract the chemically important molecular property information for the NBD system including, for example, its molecular geometry, vibrational spectra and NMR. A selection of these data, along with a comparison of them with previous work,[19−25] is given and discussed in section 5 of this paper. Finally, in section 6, conclusions from the results of the present study are drawn.

2. Experimental Details

The 18 MO's of the complete valence region of NBD, namely the $5b_2$, $7a_1$, $2a_2$, $4b_1$, $4b_2$, $6a_1$, $3b_1$, $5a_1$, $3b_2$, $2b_2$, $2b_1$, $4a_1$, $1a_2$, $3a_1$, $2a_1$, $1b_1$, $1b_2$ and $1a_1$ MO's, were investigated in several experimental runs using the Flinders symmetric noncoplanar HREMS spectrometer (see Figure 1). Details of this coincidence spectrometer and the method of taking the data can be found in Brunger and Adcock[1] and Weigold and McCarthy[2], and so we do not repeat them again here.

The high-purity NBD is admitted into the target chamber through a capillary tube, the flow rate being controlled by a variable leak valve. Note that the NBD driving pressure was too low to cause any significant clustering by supersonic expansion. The collision region is differentially pumped by a 700 Ls^{-1} diffusion pump. Apertures and slits are cut in the collision chamber for the incident beam and the scattered and ejected electrons. This differentially pumped collision region makes it possible to increase the target gas density by a factor of about 3 while keeping the background pressure in the spectrometer below 10^{-5} Torr. This was important as it enabled us to maintain workable coincidence count rate levels, even with the smaller electron beam current output from the $(e,2e)$ monochromator (typically 25 μA in this work) compared to that of a normal electron gun.[29] The coincident energy resolution of the present measurements was typically 0.55 eV (fwhm), as determined from measurements of the binding-energy (ϵ_f) spectrum of helium. However, due to the natural-line widths of the various transitions (ranging from 0.45 to 0.89 eV), as estimated from the relevant PES spectra,[10,11] the fitted resolutions of the spectral peaks for NBD varied from 0.71 to 1.05 eV (fwhm). It is precisely this limitation which forces us to combine our measured $2a_2$ and $4b_1$ orbital MDs, $3b_1$ and $5a_1$ orbital MDs, $2b_1$ and $4a_1$ orbital MDs, $1a_2$ and $3a_1$ orbital MDs and $2a_1$ and $1b_1$ orbital MDs, respectively. To do otherwise would have raised serious questions as to the uniqueness of the MDs derived in the fit (see below). The angular resolution, which determines the momentum resolution (see eq 1), was typically 1.2° (fwhm), as determined from the electron optics and apertures and from a consideration of the argon $3p$ angular correlation.

In the current study, noncoplanar symmetric kinematics were employed, that is, the outgoing electron energies E_A and E_B were equal, the scattered (A) and ejected (B) electrons made equal polar angles $\theta = 45°$ with respect to the direction of the

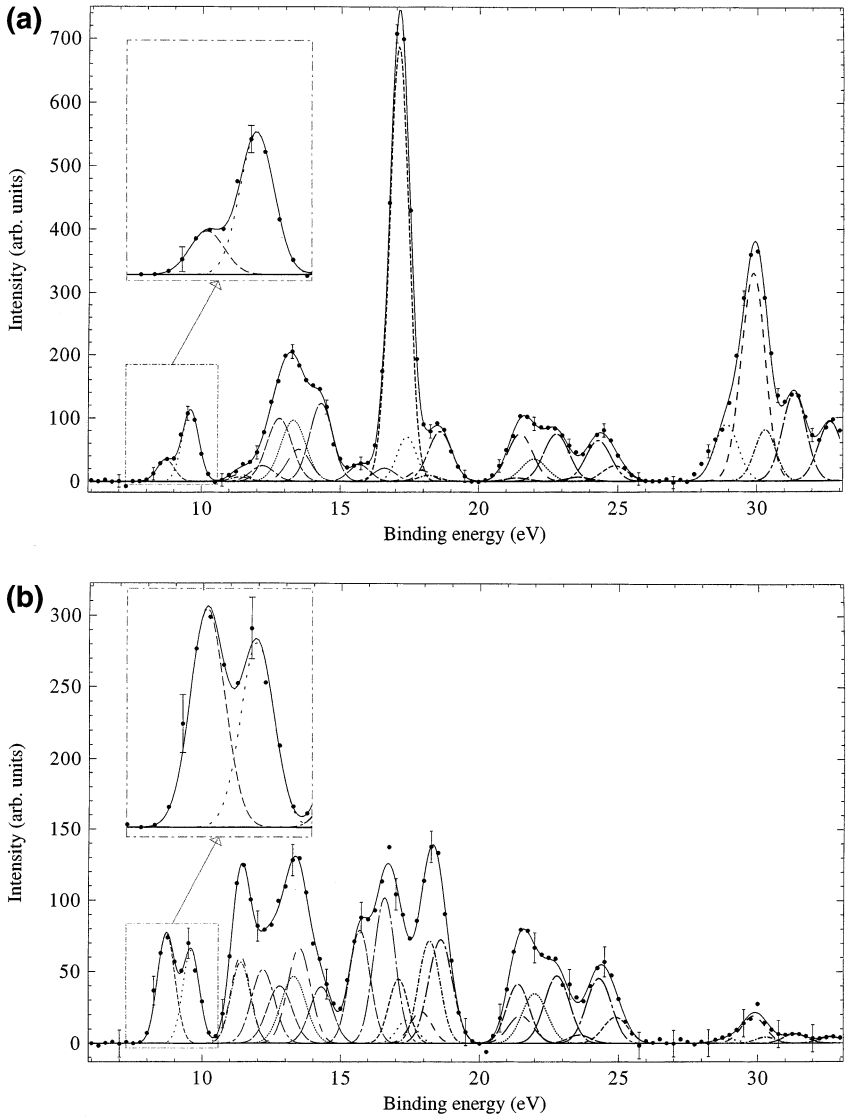

Figure 2. Typical binding-energy spectra from our 1500 eV noncoplanar symmetric HREMS investigation into norbornadiene. The curves show the fits to the spectra at (a) $\phi = 0°$($p \approx 0.03$ au) and (b) $\phi = 10°$($p \approx 0.92$ au) using the known energy resolution.

incident electrons (see Figure 1). The energy (E), $E = E_0 - \epsilon_f = E_A + E_B$, was 1500 eV. The binding-energy range of interest ($\epsilon_f = 6-33$ eV) is stepped through sequentially at each of a chosen set of angles ϕ using a binning mode[29] through the entire set of azimuthal angles ($\phi = 0-27.5°$). Scanning through a range of ϕ is equivalent to sampling different target electron momenta $\boldsymbol{p}$ as

$$p = \left[(2p_A\cos\theta - p_0)^2 + 4p^2{}_A\sin^2\theta\sin^2\left(\frac{\phi}{2}\right)\right]^{1/2} \qquad (1)$$

For zero binding energy ($\epsilon_f = 0$ eV), $\phi = 0°$ corresponds to $p = 0$ au, and for the present binding energies, angular resolution and kinematics, $\phi = 0°$ corresponds to $p \approx 0.03$ au. Similarly for $\phi = 10°$, $p \approx 0.92$ au. (Note 1au $\equiv 1a^{-1}{}_o$, where a_o = Bohr radius).

Typical binding-energy spectra[9] for NBD are given in Figure 2a,b. The solid curve in each panel represents the envelope of the 28 fitted Gaussians (various dashed curves) whose positions below $\epsilon_f = 23.0$ eV are taken from the available high-resolution PES data.[10,11] It is clear from Figure 2 that the fits to the measured binding-energy spectra are excellent. The least-squares-fit deconvolution technique used in the analysis of these spectra is based on the work of Bevington and Robinson,[30] to whom readers are referred for more detail. Above $\epsilon_f \approx 23.0$ eV, for the inner valence $1b_2$ and $1a_1$ orbitals, there are no PES data available to aid us in our fitting of the binding-energy spectra. Under these circumstances, the positions and widths of the Gaussian peaks, and the number of Gaussians, used in the spectral deconvolution were simply determined by their utility in best fitting the observed data for all ϕ. The fact that the inner valence $1b_2$ orbital needed 3 Gaussians, and the innermost valence $1a_1$ orbital needed 5 Gaussians, to incorporate the measured coincidence intensity into the fit, is possibly indicative of the existence of final state correlation interaction (FSCI) effects in the inner valence region of NBD. Alternatively, such an observation is also consistent with the natural line profiles for these orbitals being highly asymmetric. However, our previous experience with [1.1.1] propellane[31] and cubane[32] strongly suggests that our present binding-energy spectra measurements are indicative of FSCI effects being prevalent.

A sample of high-purity norbornadiene (~1.0 g) was commercially purchased (Aldrich) and distilled under N_2 to ensure high purity. In addition, it was degassed in situ by repeated freeze−pump−thaw cycles before being introduced into the interaction region. Comparing our $\phi = 0° + 10°$ binding-energy spectrum with the PES results of Bischof et al.[11] shows that

the level of qualitative agreement between them is very good. This is strong evidence for the purity of our NBD sample, an important consideration given the high sensitivity of HREMS to the presence of any impurities.

3. Theoretical Analysis

The PWIA is used to analyze the measured cross sections for high-momentum transfer (e,2e) collisions. Using the Born−Oppenheimer approximation for the target and ion wave functions, the EMS differential cross section σ, for randomly oriented molecules and unresolved rotational and vibrational states, is given by

$$\sigma = K\int d\Omega| < p\psi_f^{N-1}|\psi_i^N > |^2 \qquad (2)$$

where K is a kinematical factor which is essentially constant in the present experimental arrangement, ψ_f^{N-1} and ψ_i^N are the electronic many-body wave functions for the final [$(N-1)$ electron] ion and target [N electron] ground states, and p is the momentum of the target (NBD) electron at the instant of ionization. The $\int d\Omega$ denotes an integral over all angles (spherical averaging) due to averaging over all initial rotational states. The average over the initial vibrational state is well approximated by evaluating orbitals at the equilibrium geometry of the molecule. Final rotational and vibrational states are eliminated by closure.[2]

The momentum space target-ion overlap $< p\psi_f^{N-1}|\psi_i^N >$ can be evaluated using configuration interaction descriptions of the many-body wave functions,[33] but usually, the weak coupling approximation[29] is made. Here, the target-ion overlap is replaced by the relevant orbital of, typically, the Hartree−Fock or Kohn−Sham[34] ground state Φ_0, multiplied by a spectroscopic amplitude. With these approximations eq 2 reduces to

$$\sigma = KS_j^{(f)}\int d\Omega|\phi_j(p)|^2 \qquad (3)$$

where $\phi_j(p)$ is the momentum space orbital. Note that the relaxation of the final state has been neglected in this approximation. The spectroscopic factor $S_j^{(f)}$ is the square of the spectroscopic amplitude for orbital j and ion state f. It satisfies the sum rule

$$\sum_f S_j^{(f)} = 1 \qquad (4)$$

Hence $S_j^{(f)}$ may be considered as the probability of finding the one-hole configuration in the many-body wave function of the ion.

The Kohn−Sham equation[34] of DFT may be considered as an approximate quasiparticle equation, with the potential operator approximated by the exchange-correlation potential.[33] Usually, this is done at the local density approximation (LDA) level (also known as the local spin density (LSD) approximation), although in this study we concentrate on approximating the exchange-correlation (XC) functional with functionals that depend on the gradient of the charge density[35−38] (i.e., the GGA). Specifically, here we employed two different approximations to the XC energy functional due to Becke and Perdew (BP) and Becke, Lee, Yang, and Parr (BLYP). To compute the coordinate space Kohn−Sham orbitals ψ_j, we employed DGauss, a program package developed at CRAY Research by Andzelm and colleagues.[27,28] Note that our rationale for using DFT/DGauss over other available packages such as HF/GAUSSIAN has been considered elsewhere,[39] and so we do not repeat those details again here. DGauss is itself a part of UniChem, a suite of computational quantum-chemistry programs from PHARMACOPEIA. Employing the UniChem user interface, we built a model NBD molecule and then employed DGauss with various GGA and basis sets to minimize the total energy of NBD in its ground electronic state. The electronic structural calculations using RHF/6-31G** are based on GAMESS. A comparison of the present total energy for NBD, as calculated using our BP/TZVP XC functional and basis set, and the results from other calculations[40−42] is given in Table 1. Clearly, the present total energy compares favorably to those obtained by other workers,[40−42] who employed different degrees of sophistication in their respective basis sets. Information of the molecular structure and the molecular orbital wave functions for the ground electronic state of NBD, obtained from the DFT calculations, were next treated as input to the Flinders-developed program AMOLD,[29] which computes the momentum space spherically averaged molecular-structure factor[43] and the (e,2e) cross section or MD (see eq 3).

TABLE 1: Total Energy (in Hartrees) of NBD from This Work, Compared with Other MO Studies

ref	origin	total energy (Hartrees)
40	MP2/6-31G*	−270.553169
40	MP4//MP2/6-31G*	−270.644231
40	CCSD//MP2/6-31G*	−270.644663
41	G2/MP2	−270.93475
41	G2	−270.93386
42	G2	−270.93385
42	G2/MP2	−270.92881
42	G2/MP2, SVP	−270.92940
42	G3/MP2	−270.98953
42	B3LYP	−271.43725
present	BP/TZVP	−271.576907
present	RHF/6-31G**	−269.666160

The comparisons of calculated MDs with experiment (see section 4) may be viewed as an exceptionally detailed test of the quality of the basis set. From our previous experience,[9,31,32] the GGA-DFT method using the BP XC functional gives good agreement with the experimental MDs, compared to other GGA methods available. As a result, GGA-BP is used in combination with three basis sets to examine the behavior of the basis sets. These basis sets are denoted by the acronyms DZVP, DZVP2, and TZVP. The notations DZ and TZ denote basis sets of double- or triple-zeta quality. V denotes a calculation in which such a basis is used only for the valence orbitals and a minimal basis is used for the less chemically reactive core orbitals. The inclusion of long-range polarization functions is denoted by P. All the calculations were performed on an SGI−R500−02 work station and a CRAY J90se/82048 computer employing the computer distribution technique. Note that the term computer distribution technique is simply a shorthand notation to denote that the calculations were set up on the SGI-2 work station before being launched on the CRAY supercomputer.

4. Comparison between Experimental and Theoretical Momentum Distributions

Typical binding-energy spectra of C_7H_8 in the region 6−33 eV and at $E = 1500$ eV are given in Figure 2. These spectra were measured at each of a chosen set of angles ϕ and then analyzed with a least-squares-fit deconvolution technique.[30] This analysis then allowed us to derive the required MDs for all of the respective valence orbitals of NBD. Although the measured MDs are not absolute, relative magnitudes for the different transitions are obtained.[29] In the current HREMS investigation

of the valence states of NBD, the experimental MDs are placed on an absolute scale by summing the experimental flux for each measured ϕ for the first nine outer valence orbitals, and then normalizing this to the corresponding sum from the results of our PWIA-BP/TZVP calculation.

The results from this process for the HOMO ($5b_2$) and NHOMO ($7a_1$) orbitals were described previously by Mackenzie-Ross et al.[9] As a consequence, we do not need to repeat them in detail again here. Briefly, however, Mackenzie-Ross et al.[9] found that their experimental MDs for both the HOMO and NHOMO were generally in good accord with their corresponding PWIA-BP/DZVP, −BP/DZVP2, −BP/TZVP, and −BLYP/TZVP computations. The only exception to this observation was that their $7a_1$ theoretical MD with BP/DZVP XC functional and basis set tended to somewhat underestimate the magnitude of the (*e*,2*e*) cross section for $p \leq 0.4\ a_0^{-1}$, thereby suggesting a limitation with the accuracy of BP/DZVP. Mackenzie-Ross et al.[9] also compared the HOMO and NHOMO MD data against the respective earlier low-resolution EMS results from Takahashi et al.[18] They found that although the earlier MD data[18] exhibited more scatter and had larger uncertainties, it was still in good quantitative accord with their measurement.[9] The final observation we make in regard to NBD's HOMO and NHOMO MDs, is that in both cases there is a local minimum in the PWIA-DFT results for $p \approx 0.1\ a_0^{-1}$. The experimental MD data of Mackenzie-Ross et al.[9] provided some support for the existence of these local minima, which we believe arise due to electron correlation effects.[4]

Of NBD's 16 remaining valence orbitals, calculated and measured MDs were determined for the respective $2a_2 + 4b_1$, $4b_2$, $6a_1$, $3b_1 + 5a_1$, $3b_2$, $2b_2$, $2b_1 + 4a_1$, $1a_2$, $+ 3a_1$, $2a_1 + 1b_1$, $1b_2$, and $1a_1$ orbitals. This represents a significant volume of data, far too much to be discussed in the bulk of the text. Hence, we restrict our specific discussion to four exemplary cases ($6a_1$, $3b_2$, $2b_2$, and $1a_1$ orbital MDs), with figures for the remainder of our MDs being provided in the Supporting Information (see later).

In Figure 3, we present our 1500 eV symmetric noncoplanar MD for the $6a_1$ outer valence orbital of NBD. The shape of the present experimental $6a_1$ MD is interesting, with three local maxima observed at $p \approx 0.03$ au, $p \approx 0.28$ au, and $p \approx 1.25$ au. This result is in good qualitative agreement with each of our PWIA-BLYP/TZVP, −BP/TZVP, −BP/DZVP2, and −BP/DZVP calculations. Indeed, the shapes of all of the computations and that of the experimental MD are in good accord over the entire range of target electron momentum (*p*). However, when the magnitude of the MDs are considered, particularly at $p <$ 0.5 au, as expected the PWIA-BLYP/TZVP and PWIA-BP/TZVP calculations provide a better representation of the experimental result than either of PWIA-BP/DZVP2 or PWIA-BP/DZVP. This is indicative for BLYP/TZVP and BP/TZVP providing a more physically accurate description for the $6a_1$ orbital, compared to both BP/DZVP2 and BP/DZVP. Note that we have increased the confidence of the validity of the present experimental $6a_1$ HREMS data because the results from our two independent runs (denoted as Present Data A and Present Data B) are in very good agreement with one another.

All of the PWIA-DFT calculations predict a $3b_2$ orbital MD which is similar in shape to that just described for the $6a_1$ orbital (see Figure 4a). We note, however, that here the strength of the second local maximum in the MD (at $p \approx 0.28$ au) relative to that for the third local maximum (at $p \approx 1.15$ au), is stronger for the $3b_2$ orbital compared to that calculated previously for the $6a_1$ orbital. In addition, when compared to the measured

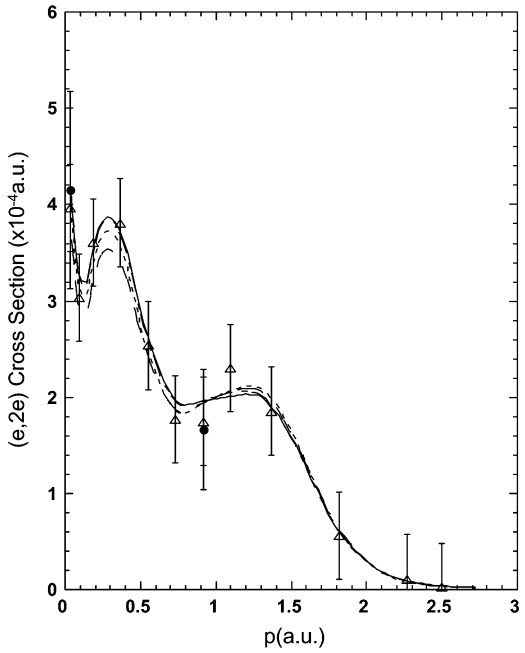

Figure 3. 1500 eV Symmetric noncoplanar MD for the $6a_1$ orbital of norbornadiene ($\epsilon_f = 12.8$ eV). The present data for Run A (●) and Run B (△) are compared against the results of our PWIA-DFT calculations: (- -) BLYP/TZVP, (—) BP/TZVP, (- - - -) BP/DZVP2, and (— —) BP/DZVP. Acronyms are defined in the text.

$3b_2$ MD, the agreement between our calculated PWIA-DFT MDs, and the HREMS experimental result is not as impressive for $3b_2$ (see Figure 4a) as it was for the $6a_1$ orbital MD (see also Figure 3). This is particularly true at $p \approx 0.04$ au where all the computations overestimate the magnitude of the experimental cross section. As the small momentum region corresponds to the large *r* (coordinate space) region of the wave function, this indicates that diffuse functions may be required in the basis sets. Notwithstanding this, Figure 4a strongly suggests, especially for $p < 0.4$ au, that the PWIA-DFT calculation with BP/TZVP basis does best in reproducing the experimental MD. This latter observation is also totally consistent with what we found above for the $6a_1$ orbital. Finally, we note the good agreement between the measured $3b_2$ cross sections that we obtained in our two independent experiments.

In Figure 5a we plot the present experimental and theoretical MDs for the inner valence $2b_2$ orbital of NBD. The $2b_2$ orbital has the same symmetry as the $3b_2$ orbital we just discussed, but it is apparent from Figure 5a that the resulting experimental and calculated $2b_2$ MDs are very different in shape to that which we found for the $3b_2$ orbital. This difference indicates that the bonding mechanisms of the two MOs are not the same, the EMS MDs indicating that the $3b_2$ MO has more CI, whereas the $2b_2$ MO has a more π-like MD. This latter observation is proven by the respective MO wave functions given by Figures 4b and 5b from our ab initio RHF calculation. The difference in the $3b_2$ and $2b_2$ MDs also highlights the sensitivity of HREMS in differentiating between different orbitals of the same symmetry, a very useful property when questions pertaining to the correct ordering (in terms of binding energy) of the orbitals arise. In this case, all the PWIA-DFT $2b_2$ computations overestimate the magnitude of the measured MD (see Figure 5a). However when our PWIA-BP/TZVP momentum distribution is scaled by a factor of 0.85, agreement in terms of the shape and magnitude between this scaled MD and the measured $2b_2$ MD is now very good, across the entire range of measured *p*. This observation simply reflects that the spectroscopic factor for the $2b_2$ orbital,

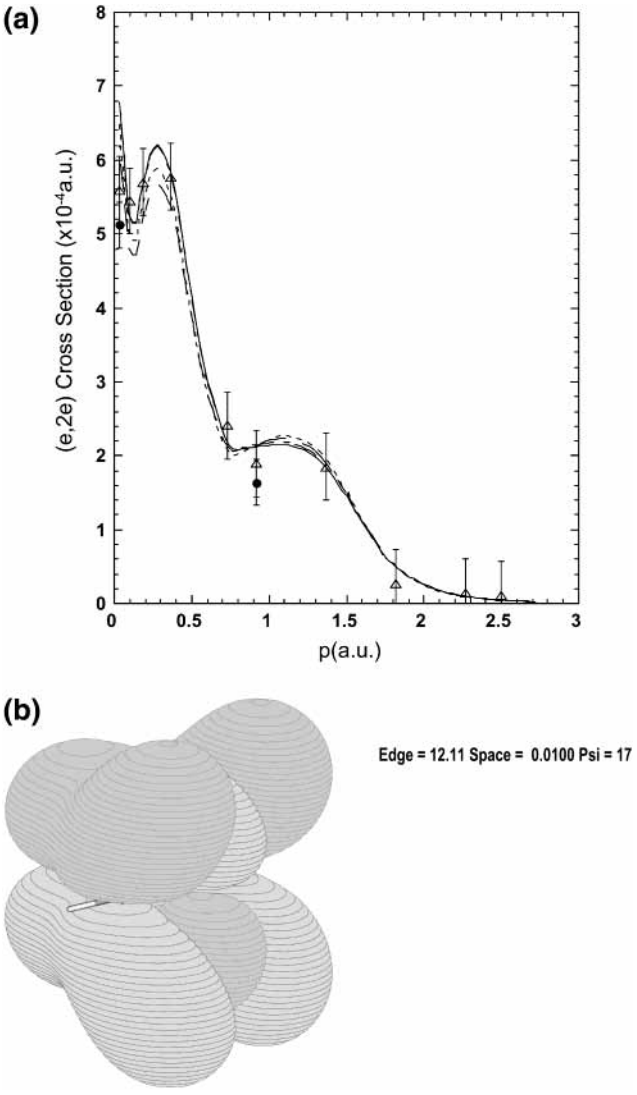

Figure 4. (a) The 1500 eV symmetric noncoplanar MD for the $3b_2$ orbital of norbornadiene ($\epsilon_f = 14.3$ eV). The legend is the same as that for Figure 3. (b) Contour plot of the $3b_2$ MO wave function from our RHF/6-31G** calculation.

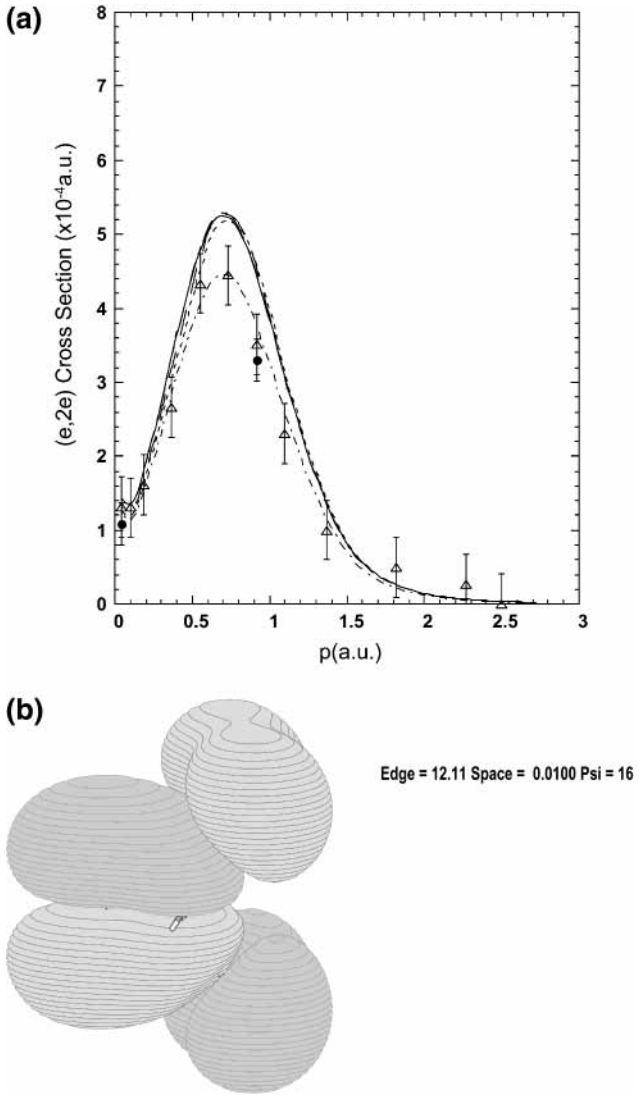

Figure 5. (a) The 1500 eV symmetric noncoplanar MD for the $2b_2$ orbital of norbornadiene ($\epsilon_f = 15.7$ eV). The legend is the same as that for Figure 3 except (- - − - - -) represents the 0.85 × PWIA − BP/TZVP result. (b) Contour plot of the $2b_2$ MO wave function from our RHF/6-31G** calculation.

at the relevant $2b_2$ binding energy ($\epsilon_f = 15.7$ eV), is $S_{2b_2} = 0.85$. Note that the missing (see eq 4) 15% $2b_2$ spectral flux must be found somewhere else in the measured binding energy spectra of Figure 2, or at higher binding energies outside the range of the present measurement. Up until now, the spectroscopic factors for each of the $5b_2$, $7a_1$, $2a_2$, $4b_1$, $4b_2$, $6a_1$, $3b_1$, $5a_1$, and $3b_2$ orbitals, at their respective relevant binding energies, have all been $S_j^{(f)} \approx 1$. The fact that from now on the spectral strength of a given orbital might be split, probably due to final-state-configuration-interaction effects[2], at a number of binding energies, may significantly complicate the interpretation of the measured MDs. This in turn would make the comparison between our calculated and experimental MDs not straightforward. Representative cases where this effect is discussed, and our response to it, can be found in Brunger and Adcock.[1]

The final orbital we specifically discuss is the innermost valence $1a_1$ orbital. Our calculated PWIA-DFT MDs and our measured MD (taken from peaks 24−28 of Figure 2), for this orbital, are plotted in Figure 6. Here, we find that there is only qualitative agreement between all our PWIA-DFT calculations and the experimental MD, the theory drastically overestimating the strength of the cross section at $p \leq 0.9$ au and thereafter underestimating the magnitude of the cross section. Similar behavior had been previously observed[2] in the inner valence region of the rare gases, where it was found that a distorted wave description, as distinct from the PWIA, of the ionization process was necessary to correctly reproduce the measured MDs. Another possible explanation for the discrepancy in Figure 6 is that FSCI effects lead to both a splitting and a mixing of the inner valence $1a_1$ and $1b_2$ orbitals. This hypothesis was tested by also plotting the hybrid MD ($0.55 \times 1a_1 + 0.20 \times 1b_2$), with BP/TZVP basis, in Figure 6. Agreement between this hybrid MD and the experimental MD is now very good for $p \leq 0.9$ au, but for $p > 0.9$ au a discrepancy still remains which further suggests a distorted wave description for the reaction mechanism really is necessary here. Note that possible distortion effects in molecular systems has been discussed recently by Brion et al.[4] Evidence supporting the notion that the $1a_1$ and $1b_2$ spectral strength is split can be gleaned from our binding energy spectra (see Figure 2). At both $\phi = 0°$ and $\phi = 10°$, there is clearly nonzero intensity in these spectra around $\epsilon_f = 33$ eV, strongly suggesting that further real spectral strength, of $1a_1$ and $1b_2$ origin, does exist outside our measured binding energy range. Further note, that theoretical evidence for the splitting in spectral strength for the inner valence region in larger

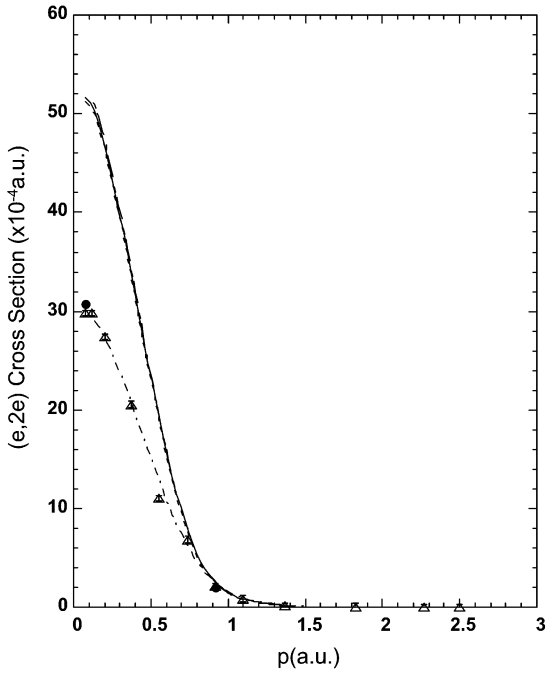

Figure 6. 1500 eV Symmetric noncoplanar MD for the $1a_1$ orbital of norbornadiene ($\epsilon_f \geq 28$ eV). The legend is the same as that for Figure 3 except (- - − - - -) represents ($0.55 \times 1a_1$ MD $+0.20 \times 1b_2$ MD) for BP/TZVP.

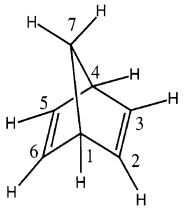

Figure 7. Structural representation of norbornadiene.

molecules comes from high-level Green's function calculations (see e.g., refs 31 and 32) and our ab initio RHF calculation which predicts that the innermost valence $1a_1$ MO has a binding energy of 32.19 eV.

In summary, when the measured and calculated MDs that we studied (see Figures 3−6 and the Supporting Information) are compared in detail, we find that the best overall description of the respective experimental MDs is provided by the TZVP basis. There is, however, no significant difference in the quality of the calculated MDs when either the BLYP or BP exchange correlation functional is employed. After very careful further consideration the PWIA-BP/TZVP results are probably marginally superior, although with the statistical errors of the present data we cannot be more definitive in this case.

5. Molecular Property Information

Experimental validation of Hartree−Fock or DFT basis sets using HREMS may provide a route to appropriate basis sets for calculating other types of molecular properties, such as molecular geometries, charge distributions, and orbital energies. Previous work[40−42,19−23] has used a variety of MO approaches to determine structural and electronic properties of NBD. We took our "optimum" BP/TZVP basis set and used it to derive some of these molecular properties.

5.1 Molecular Geometries. In Figure 7, we provide a structural representation of the norbornadiene molecule. Also defined in this figure are the C-sites that are referred to extensively in Table 2 and in the discussion that follows.

TABLE 2: Comparison between the Present BP/TZVP Results and the Results of Other Calculations[21−23] and Experiments[19,20] for the Molecular Geometry of Norbornadiene

parameter	FTMW[19]	ED[20]	present	3-21G[21,22]	6-31G*[23]
r(C1−C2)/Å	1.5304 (31)	1.5332 (14)	1.546	1.550	1.5395
r(C1−C7)/Å	1.5567 (28)	1.5711 (31)	1.563	1.566	1.5505
r(C2−C3)/Å	1.3362 (30)	1.3387 (12)	1.341	1.319	1.3192
r(C1−H)/Å	1.0903 (13)	1.1094 (47)	1.097	1.076	
r(C2−H)/Å	1.0809 (13)	1.0896 (47)	1.090	1.069	
r(C7−H)/Å	1.0954 (12)	1.1094 (47)	1.101	1.081	
∠C1C2C3/°	107.13 (9)		107.14	107.5	
∠C1C7C4/°	91.90 (17)	92.2 (4)	92.256	92.0	91.87
∠C2C1C6/°	107.58 (25)		107.06	106.2	107.45
∠C2C1C7/°	98.30 (14)		98.37	98.3	98.31
∠C7C1H/°	117.66 (26)		117.82	118.2	
∠C3C2H/°	127.84 (10)	125.2 (14)	127.78	128.1	
∠HC7H′/°	111.99 (14)	114.7 (30)	110.9	111.7	
d(C2...C6)/Å	2.473	2.462	2.487	-	

In general, we find that our calculation of NBD's molecular geometries was in very good agreement with other experimentally determined geometries[19,20] and also they compared favorably with the results from other MO calculations.[21−23] Some of these results are summarized in Table 2. In particular, our bridgehead carbon−carbon distance of 1.563 Å is in excellent agreement with the two most accurate experimental values of 1.557 Å from a Fourier transform microwave (FTMW) study[19] and a value of 1.571 Å from an electron diffraction (ED) study.[20] The carbon−carbon double bond lengths were 1.341 Å from our BP/TZVP calculation, compared with 1.3362(30) Å from FTMW and 1.3387(12) Å from ED. The nonbridgehead single-bond lengths were slightly overestimated by BP/TZVP compared with experiment (see Table 2), but this was a smaller error than that from earlier SCF 3-21G calculations[21,22] and an SCF 6-31G* calculation.[23] The distance between the two double bonds was particularly well reproduced by our BP/TZVP calculation, with the C2 .... C6 distance being 2.487 Å compared with the experimental distance of 2.473 Å (FTMW) and 2.462 Å (ED). Trends in the C−H bond lengths determined in the FTMW study[19] were also reproduced by our BP/TZVP, with the experimental values typically being 0.007 Å smaller than the theory results.

It is also apparent from Table 2 that the respective bond angles of NBD are well reproduced by our calculation. In particular, the C1C2C3 bond angle is measured by FTMW to be 107.13(9)°, which is accurately predicted by the present calculation of 107.14°. Similarly, the bond angle C7C1H is given by FTMW to be 117.66(26)°, again in good agreement with our prediction of 117.82°.

5.2 Electronic Properties. The accidentally small dipole moment of NBD is reproduced very well by our BP/TZVP DFT calculation. We obtain a value of 0.082D from our computation, compared with the very accurate FTMW value of 0.05866(9)D. Our BP/TZVP calculations of charges fitted to the electrostatic potential was considered to be the most realistic estimate of atom charges. These values are given in Table 3, where the Mulliken and Lowdin charges are also included for the purpose of comparison.

It is of particular interest to investigate the electron density in the carbon−carbon region of NBD. We carried out a study analogous to that of Wiberg and co-workers,[44] to estimate the electron density (ρ) at the bond critical point (midway betwen the two carbons). We obtained a value of $\rho_b = 0.3282a_0^{-3}$ for the double bonds and $0.2266a_0^{-3}$ for the single bonds. We also used Wiberg's empirical method to calculate bond orders from electron densities at the bond critical points, as derived from

TABLE 3: Atom Charges of NBD from the BP/TZVP DFT Calculation

atom	charge fitted to electrostatic potential	Mulliken charges	Lowdin charges
C2, C3, C5, C6	−0.242	−0.128	−0.123
C1, C4	+0.307	−0.125	−0.118
C7	−0.354	−0.224	−0.135
(C7)−H	+0.095	+0.129	+0.104
(C1)−H, (C4)−H	−0.004	+0.121	+0.103
(C2)−H etc.	+0.131	+0.121	+0.113

our BP/TZVP computation. The electron densities at the bond critical points of the model compounds ethane, ethene, ethyne, and benzene (bond orders of 1.0, 2.0, 3.0, and 1.5) were used to determine the constants in the relation between bond order n and the bond critical point electron densities ρ_b

$$n = \exp\{7.004\,(\rho_b - 0.224)\}$$

This relationship yielded a bond order for the carbon−carbon bonds in NBD of 1.90 for the double bonds and 0.924 for the single bonds. We also calculated the bond order of the carbon−carbon bonds using Mulliken and Mayer populations analysis. The Mayer bond order of 1.90 for the double bonds and 0.95 for the single bonds was in good agreement with our respective values. The Mulliken value of 1.32 for the double bonds and 0.73 for the single bonds reflects the well-known deficiencies of this method of orbital decomposition.

5.3 Vibrational Spectra. There have been a number of experimental determinations of the vibrational spectra of norbornadiene, both infrared and Raman. These results are summarized in Kawai et al.[24] Our BP/TZVP density functional computations were able to calculate the frequencies of the vibrational modes of NBD with reasonable accuracy, as shown in Table 4 where the present calculated vibrational frequencies are compared with the experimental IR and Raman spectroscopy results.[24] Also shown in this table are the assignments for the various vibrational modes, where we have followed the work of Levin et al.[45] and Shaw et al.[46] Finally, we also compare in Table 4 the calculated and experimental intensities of the transitions. It is again clear from this table that our BP/TZVP results are in quite good accord with the observed experimental spectra.

TABLE 4: Calculated (using BP/TZVP) and Experimental[24] Vibrational Frequencies (cm^{-1}) and Intensities (km/mol) of Norbornadiene

BP/TZVP spectrum			experimental spectrum[24]		
mode	frequency (cm^{-1})	intensity (km/mol)	frequency (cm^{-1})	intensity	assignment[45,46]
7	404.59	9.43	425	m	a1, v12
8	449.83	0.00	446		a2, v20
9	487.02	9.02	502	m	b2, v39
10	537.03	1.11	542	w	b1, v30
11	628.14	40.87	668	s	b2, v38
12	705.85	0.00		w	
13	717.29	60.32	728	vs	a1, v11
14	768.09	4.13	774	m	a1, v10
15	799.30	9.69	800	m	b1, v29
16	846.40	2.47	874	w	a1, v9
17	867.37	6.32	879	m	b1, v28
18	871.89	1.06			
19	875.79	1.24	889	w	a2, v18
20	895.28	0.08	877	w	a1, v9
					b1, v28
21	918.85	2.15	895	m−w	b2, v37
22	932.84	4.51	915	m	b1, v27
23	945.80	0.07	938	vw	a1, v8
24	1003.60	0.63	950	w	b1, v26
25	1056.60	1.34	1017	w	b2, v36
26	1089.12	0.14	1066	w	b2, v35
27	1098.96	0.03	1103	w	a1, v7
28	1138.61	1.85	1111	m	a2, v16
29	1172.97	4.13	1152	w−m	b1, v25
30	1211.76	0.01			
31	1216.82	5.18	1204	m	b2, v34
32	1229.76	0.21	1229	m	a1, v6
33	1249.98	0.10	1240	w	
34	1301.20	26.90	1270	s	a2, v14
			1308		b1, v24
					b1, v23
35	1454.53	2.60	1450	w	a1, v5
36	1557.34	10.36	1556	s	a1, v4
			1568		
			1575		
37	1599.82	0.36	1603	w	
38	2981.27	42.50	2934	s	a1, v3
39	3042.45	28.53	2987	s	a1, v2
40	3050.29	39.55	3001	s	b2, v32
41	3051.31	18.93	3060	s	a1, v1
42	3132.11	2.08	3073	m	b1, v21
43	3135.75	0.63	3102	w	a1, v1
44	3154.94	1.34	3123	w	b2, v32
45	3159.22	0.70	3146	w	A1

Assignment of the vibrational modes follows the work of Levin et al.[45] and Shaw et al.[46]

6. Conclusions

We have reported on the first comprehensive HREMS study into the complete valence electronic structure of norbornadiene. MDs for the $5b_2$, $7a_1$, $2a_2 + 4b_1$, $4b_2$, $6a_1$, $3b_1 + 5a_1$, $3b_2$, $2b_2$, $2b_1 + 4a_1$, $1a_2 + 3a_1$, $2a_1 + 1b_1$, $1b_2$, and $1a_1$ orbitals were measured and compared against a series of PWIA-based calculations using DFT basis sets. Our calculations, for each of the three basis sets (DZVP, DZVP2, TZVP), were performed using both BP and BLYP exchange correlation corrections to the DFT functional. On the basis of this comparison between the experimental and theoretical MDs, we found that BP/TZVP provided the most physically reasonable representation of the NBD wave function. Molecular property information derived from this "optimum" BP/TZVP basis was seen to be in good agreement with the corresponding results from independent measurements. This provides compelling evidence for the pedigree of HREMS in a priori basis set evaluation.

Future studies will now concentrate on the respective electronic structures of norbornene (C_7H_{10}) and norbornane (C_7H_{12}). We propose this investigation in order to probe how the electronic structure of these molecules changes as the double bonds of NBD are progressively saturated. Are there any discernible trends, particularly in the momentum distributions, and if so can we quantify them in a logical manner. In addition, we note that an improvement in the reaction mechanism description, particularly for inner valence and core states, by the development of a distorted wave framework[2] for multicentered targets (i.e., molecules) would be desirable. A small step in this regard was recently made by Champion et al.,[47] although we note that exchange was neglected in their work, the scattering potentials were effectively approximated as being central, distortion was only included for the ejected electron, and it is also not clear whether convergence under HREMS kinematical conditions would be achieved.

Acknowledgment. This work was supported in part by the Australian Research Council, and we thank Ms Marilyn Mitchell for typing the manuscript. One of us (W.R.N.) also thanks the

Flinders University of South Australia for its hospitality during his visit there. F.W. thanks Dr. H. Quiney for useful discussions.

Supporting Information Available: Momentum distributions for the remaining $2a_2 + 4b_1$, $4b_2$, $3b_1 + 5a_1$, $2b_1 + 4a_1$, $1a_2 + 3a_1$, $2a_1 + 1b_1$, and $1b_2$ orbitals of NBD are respectively presented in Figures 8-14. This material is available free of charge via the Internet at http://pubs.acs.org.

References and Notes

(1) Brunger, M. J.; Adcock, W. *J. Chem. Soc., Perkins Trans. 2* **2002**, 1−22.
(2) Weigold, E.; McCarthy, I. E. *Electron Momentum Spectroscopy*; Kluwer Academic/Plenum Publishers: New York, 1999.
(3) Frost, L.; Weigold, E. *J. Phys. B* **1982**, *15*, 2531.
(4) Brion, C. E.; Cooper, G.; Feng, R.; Tixier, S.; Zheng, Y.; McCarthy, I. E.; Shi, Z.; Wolfe, S. In *Correlations, Polarization and Ionisation in Atomic Systems*; Madison, D. H., Schulz, M., Eds; AIP Conference Proceeding 604, 2002; pp 38−44.
(5) Hoffmann, R. *Acc. Chem. Res*. **1971**, *4*, 1.
(6) Hoffmann, R.; Heilbronner, E.; Gleiter, R. *J. Am. Chem. Soc*. **1970**, *92*, 706.
(7) Hoffmann, R.; Imamura, A.; Hehre, W. J. *J. Am. Chem. Soc*. **1968**, *90*, 1499.
(8) Heilbronner, E.; Schmelzer, A. *Helv. Chim. Acta* **1975**, *58*, 936.
(9) Mackenzie-Ross, H.; Brunger, M. J.; Wang, F.; Adcock, W.; Trout, N.; McCarthy, I. E.; Winkler, D. A. *J. Electron. Spectrosc. Relat. Phenom*. **2002**, 389.
(10) Bischof, P.; Hashmall, J. A.; Heilbronner, E.; Harnung, V. *Helv. Chim. Acta* **1969**, *52*, 1745.
(11) Bieri, G.; Burger, F.; Heilbronner, E.; Maier, J. P. *Helv. Chim. Acta* **1977**, *60*, 2213.
(12) von Niessen, W.; Diercksen, G. H. F. *J. Electron. Spectrosc. Relat. Phenom.* **1979**, *16*, 351.
(13) Heilbronner, E.; Martin, H. D. *Helv. Chim. Acta* **1972**, *55*, 1490.
(14) Galasso, V. *Chem. Phys.* **1989**, *138*, 231.
(15) Dewar, M. J. S.; Bodor, N.; Worley, S. D. *J. Am. Chem. Soc*. **1970**, *92*, 19.
(16) Palmer, M. H.; Findlay, R. H. *Chem. Phys. Lett*. **1972**, *15*, 416.
(17) Lindholm, E.; Fridh, C.; Asbrink, L. *Faraday Discuss. Chem. Soc*. **1972**, *54*, 127.
(18) Takahashi, M.; Ogino, R.; Udagawa, Y. *Chem. Phys. Letts*. **1998**, *288*, 714.
(19) Knuchel, G.; Grassi, G.; Vogelsanger, B.; Bauder, A. J. *Am. Chem. Soc*. **1993**, *115*, 10 845.
(20) Chiang, J. F.; Chiang, R.; Lu, K. C.; Sung, E-M.; Harmony, M. D. *J. Mol. Struct.* **1977**, *41*, 67.
(21) Paddon-Row, M. N.; Wong, S.; Jordan, K. D. *J. Am. Chem. Soc*. **1990**, *112*, 1710.
(22) Castro, C.R.; Dutler, R.; Rauk, A.; Wieser, H. *THEOCHEM* **1987**, *152*, 241.
(23) Zgierski, M. Z.; Zerbetto, F. *J. Chem. Phys*. **1993**, *98*, 14.
(24) Kawai, N. T.; Gilson, D. F. R.; Butler, I. S. *J. Phys. Chem.* **1990**, *94*, 5729.
(25) Krawczyk, K.; Szatylowicz, A.; Gryff-Keller, A. *Magn. Reson. Chem.* **1995**, *33*, 349.
(26) Kishimoto, N.; Ogasawara, H.; Ohno, K. *J. Phys. Chem*. **2002**, submitted.
(27) Andzelm, J.; Wimmer, E. *J. Chem. Phys*. **1992**, *96*, 1290.
(28) Komornicki, A.; Fitzgerald, G. J. *J. Chem. Phys.* **1993**, *98*, 1398.
(29) McCarthy, I. E.; Weigold, E. *Rep. Prog. Phys.* **1991**, *54*, 789.
(30) Bevington, P. R.; Robinson, D. K. *Data Reduction and Error Analysis for the Physical Sciences*; McGraw-Hill Inc.: New York, 1990.
(31) Adcock, W.; Brunger, M. J.; Clark, C. I.; McCarthy, I. E.; Michalewicz, M. T.; von Niessen, W.; Weigold, E.; Winkler, D. A. *J. Am. Chem. Soc*. **1997**, *119*, 2896.
(32) Adcock, W.; Brunger, M. J.; McCarthy, I. E.; Michalewicz, M. T.; von Niessen, W.; Wang, F.; Weigold, E.; Winkler, D. A. *J. Am. Chem. Soc.* **2000**, *122*, 3892.
(33) Casida, M. *Phys. Rev. A* **1995**, *51*, 2005.
(34) Kohn, W.; Sham, L. *J. Phys. Rev.* **1965**, *140*, A1133.
(35) Becke, A. D. *Phys. Rev. A* **1988**, *38*, 3098.
(36) Becke, A. D. *J. Chem. Phys*. **1988**, *88*, 2547.
(37) Perdew, J. P. *Phys. Rev. B* **1986**, *33*, 8822.
(38) Lee, C.; Parr, R. G.; Yang, W. *Phys. Rev. B* **1988**, *37*, 785.
(39) Michalewicz, M. T.; Brunger, M. J.; McCarthy, I. E.; Norling, V. M. In *CRAY Users Group 1995 Fall Proceedings*; Shaginaw, R., Ed.; 1995; pp 37−41.
(40) Bach, R. D.; Schilke, I. L.; Schlegel, H. B. *J. Org. Chem.* **1996**, *61*, 4845.
(41) Castano, O.; Notario, R.; Abboud, J-L.M.; Gomperts, R.; Palmeiro, R.; Frutos, L-M. *J. Org. Chem.* **1999**, *64*, 9015.
(42) Rogers, D. W.; McLafferty, F. J. *J. Phys. Chem. A* **1999**, *103*, 8733.
(43) McCarthy, I. E.; Weigold, E. *Rep. Prog. Phys.* **1988**, *51*, 299.
(44) Wiberg, K. B.; Bader, R. F. W.; Lau, C. C. H. *J. Am. Chem. Soc.* **1987**, *109*, 985.
(45) Levin, I. W.; Harris, W. C. *Spectrochim. Acta*. **1973**, *29A*, 1815.
(46) Shaw, R. A.; Castro, C.; Dutler, R.; Rauk, A.; Wieser, H. *J. Chem. Phys*. **1988**, *89*, 716.
(47) Champion, C.; Hanssen, J.; Hervieux, P. A. *Phys. Rev. A* **2002**, *65*, 022710.